THE JOURNAL OF PHYSICAL CHEMISTRY C

Article

pubs.acs.org/JPCC

Infrared Spectral Signatures of Multilayered Surface-Fluorinated Graphene: A Molecular Dynamics Study

Akira Ueta,[†] Yoshitaka Tanimura,[‡] and Oleg V. Prezhdo*[,‡]

[†]Department of Chemistry, Graduate School of Science, Kyoto University, Kitashirakawa, Sakyoku, Kyoto 606-8502, Japan

[‡]Department of Chemistry, University of Rochester, Rochester, New York 14627-0216, United States

ABSTRACT: Multilayered fluorinated graphene exhibits novel properties and finds applications in electrodes, membranes, thermal materials, transistors, and so on. These applications rely heavily on interlayer interactions that arise from sheet stacking. Because the properties of multilayered fluorinated graphene are very sensitive to the synthetic conditions, characterization of the graphene structure becomes particularly important. We theoretically analyzed the structure and interactions in multilayer fluorinated graphene by IR spectroscopy. Significant differences between the multiple- and single-layer signals were observed with the F−F vibrational motions around 700 cm^{-1}, because these motions are strongly affected by fluorines of neighboring layers. The intensity and profile of the F−F vibration peaks near 700 cm^{-1} change dramatically depending on the number of layers and the fluorine-addition pattern. These findings suggest that IR spectroscopy can be used for comprehensive characterization of the structure of multilayered fluorinated graphene.

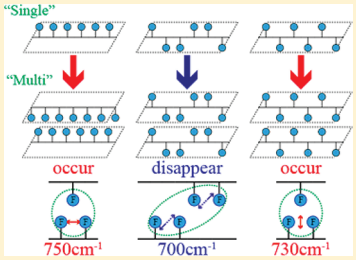

1. INTRODUCTION

Owing to sheet-stacking and interlayer interactions, multilayered functionalized carbon nanostructures, such as fluorinated multiwalled carbon nanotubes and multilayered graphene, exhibit novel physical properties that can be utilized to produce electrodes for batteries and capacitors, membranes, thermal materials, transistors, and so on.[1−10] To correlate the material's functionality with its atomic and electronic structure, a variety of investigations, employing semiempirical calculations,[1,9−11] transmission electron microscopy (TEM),[12−15] X-ray photoelectron spectroscopy (XPS),[12−16] and Raman and IR spectroscopies,[1,6,11−13,15] have been carried out. It has been found that the structures and properties of multilayered systems are strongly affected by subtle changes in the synthetic conditions.[8,17−19] Therefore, an accurate description of the multilayered architecture of nanoscale carbon carries great importance for the generation of stable and uniform structures based on well-established synthetic procedures.[6,11,13,15,19]

Using molecular dynamics (MD) simulation, the current study shows that the structure of multilayered fluorinated graphene (F−graphene) can be accurately characterized by IR spectroscopy. Specific prescriptions for distinguishing various multilayer fluorination patterns are presented and analyzed. In particular, the F−F vibrational peaks involving neighboring fluorines within the same graphene layer were found to be most suitable for characterizing interlayer interactions, because they are strongly influenced by multilayer stacking. These peaks reside in the 700−900 cm^{-1} frequency range. Different fluorination patterns are sensitive to light polarization, and therefore, they can be distinguished by collecting IR spectra polarized in different directions within the graphene plane and perpendicular to the plane.

The next section presents the theoretical approaches used in the calculations, including a discussion of the interactions potentials, details of the MD simulations, and the procedure for computing IR spectra. The section also justifies the choice of the graphene fluorination patterns selected for the current study. The calculated spectra are presented next. Particular peaks that can be used to identify considered fluorination patterns are identified, and their atomic origins are analyzed. The primary discussion focuses on single-, double-, and triple-layer graphene, and extrapolations to more layers are considered. The article ends with a summary of most important observations and a few concluding remarks.

2. THEORETICAL METHODS

This study focuses on the three fluorination patterns that are predicted to be most important for the fluorinated multilayered graphene.[1,6,20−22] The structures are illustrated in Figure 1a−c for three graphene layers. The fluorination patterns are labeled u, uudd, and ud, respectively, reflecting the sequence of upward- (u) and downward- (d) pointing fluorines. For each of these patterns, we consider single-, double-, triple-, and quadruple-layer systems. Changing the number of layers is particularly important for the u pattern, as can be seen in Figure 1a. In this case, the interlayer F−F interactions range from the strongest to the weakest of all fluorination patterns, varying significantly depending on whether the fluorines of different layers point toward and outward each other; consider pairs of layers 1−2 and 2−3.

Received: February 24, 2012
Revised: March 10, 2012
Published: March 12, 2012

   dx.doi.org/10.1021/jp301856q | J. Phys. Chem. C 2012, 116, 8343−8347

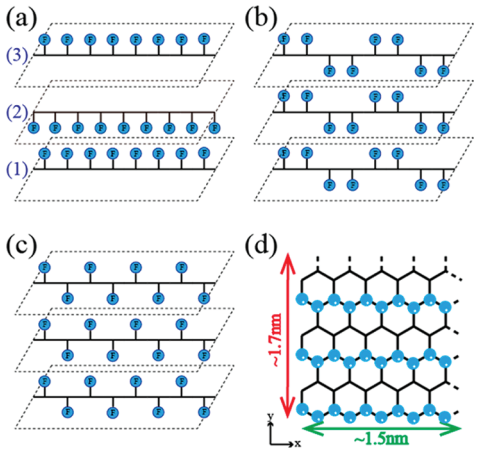

Figure 1. Fluorinated graphene systems used in this study. The fluorination patterns shown in parts a–c are labeled u, uudd, and ud, respectively, reflecting the sequence of upward- (u) and downward- (d) fluorines in each fluorine chain. Part d displays the periodic boundary of the simulation cells. The blue balls are fluorine atoms. The *x* and *y* axes are shown in part d. The *z* direction is perpendicular to the graphene plane.

Periodic boundary conditions were used (Figure 1d). The dimensions of the simulation cell in the plane of graphene were ~1.5 nm by ~1.7 nm. Each graphene layer consisted of 96 carbon atoms and 48 fluorine atoms. All three u, uudd, and ud fluorination structures, shown in Figure 1a–c, involved a 2:1 ratio of carbons to fluorines. The fluorine atoms were arranged in the 1,2-position in each benzene ring. The 1,2-addition pattern has been found to be most stable in many studies.[8,18,21–28]

The MD simulations were carried out by extending the force field employed in our earlier work.[29,30] F–graphene was generated using Brenner potentials for the intramolecular C–C, C–F, and F–F interactions[31,32] and van der Waals and electrostatic potentials for the interlayer interactions. The procedure for generating the van der Waals parameters for the Brenner potentials can be found in refs 33 and 34. To save CPU time, intramolecular interactions between atoms separated by more than four bond lengths and interlayer interactions separated by more than three interlayer distances were disregarded. Some articles have suggested[7,9] that nonbonding interaction can be significant beyond the nearest and second-nearest graphene layers. Note that our analysis focuses on comparison of single-, double-, and triple-layer systems. Therefore, neglecting four-layer and longer-distance interactions forms a good approximation for the present purposes. The velocity Verlet algorithm was used to integrate the equations of motion with a 0.1-fs time step. The simulations were performed at around 273 K. The simulation parameters, including the charges on the C and F atoms, can be found in refs 29 and 30.

The IR signal was obtained by computing the dipole autocorrelation function $\langle \mu(t)\, \mu(0)\rangle$. The Fourier transform of the correlation function is defined by

$$I_{\mathrm{MD}}(\omega) = \frac{1}{2\pi}\int_{-\infty}^{\infty} \mathrm{d}t\, \mathrm{e}^{-\mathrm{i}\omega t}\langle \mu(t)\mu(0)\rangle \qquad (1)$$

The IR spectrum $\alpha(\omega)$ is determined using the semiclassical approximation to the fully quantum-mechanical commutator $\langle[\mu(t), \mu(0)]\rangle$

$$\alpha(\omega) = \omega \tanh\left(\frac{\hbar\omega}{2k_{\mathrm{B}}T}\right) I_{\mathrm{MD}}(\omega) \qquad (2)$$

where k_{B} is the Boltzmann constant, T is the temperature, and $\hbar$ is Planck's constant.[29,30]

Three independent polarizations of light were considered during the calculation of the IR spectra. The *x* direction points along the chains of fluorine atoms obtained by the 1,2-addition (Figure 1d). The *y* direction is in the plane of the sheet and perpendicular to the fluorine chains. The *z* direction is perpendicular to the sheet. Each IR optical response function was computed by averaging over an ensemble of 10^6 different initial configurations.

3. RESULTS AND DISCUSSION

Our MD simulations show that the fluorine atoms of neighboring layers are staggered with respect to each other (Figure 1), confirming the prediction of the Daumas–Herold model.[1,6,35] The interlayer distance is about 0.6 nm, and the C–C radial distribution functions computed for all three fluorine addition patterns (results not shown) are similar to those obtained for functionalized graphite in the earlier studies.[3,6] These results indicate that our simulations are able to reproduce accurately the structures of single- and multilayered F–graphene.

The IR spectra displayed in Figures 2–4 exhibit significant differences, depending on the fluorination pattern and the number of graphene layers (Figure 1). The most significant differences are observed in the 700–850 cm^{-1} frequency range. To explore the origin of these differences, we performed a normal-mode analysis and found that the 700–900 cm^{-1} peaks originate from the F–F vibrations involving fluorine atoms bound to the same graphene layer. Interlayer interactions alter the optical activity of these vibrations. The peak around 900–1000 cm^{-1} arises from the wagging motion of F–C(sp^3) bonds, whereas the peak around 1200–1350 cm^{-1} is due to the stretching motion of the F–C(sp^3) bonds. The stretching motion of the C–C bonds is observed in the spectrum at 1000–1200 cm^{-1}. The peaks at 600 cm^{-1} and below arise from collective modes of the graphene sheet. The bottom panels of Figures 2–4 present schematic representations of the relevant vibrational modes in the most interesting frequency range between 700 and 900 cm^{-1}. In the following discussion, we analyze the effects of the interlayer interactions on the IR spectra in more detail for each of the three addition patterns.

Consider the u fluorination pattern (Figure 1a). The IR spectra computed for single- and double-layer graphene with the u fluorination pattern are shown in Figure 2. The light is polarized in the *x* direction along the fluorine chains. The most pronounced differences in the IR spectra of the single- and double-layer structures appear at 750 and 830 cm^{-1}. These peaks arise from F–F vibrations and are affected by interlayer interactions (Figure 2b). The 750 cm^{-1} peak shifts to a higher frequency in the double layer because of these interactions, and the 830 cm^{-1} vibration becomes optically active and involves mixing of the F–F and F–C(sp^3) wagging motions. The peak positions of the F–C(sp^3) wagging vibration around 900 cm^{-1} are also different for the single- and double-layer u-fluorinated graphene. The peak shifts to a higher frequency in the double-

dx.doi.org/10.1021/jp301856q | J. Phys. Chem. C 2012, 116, 8343–8347

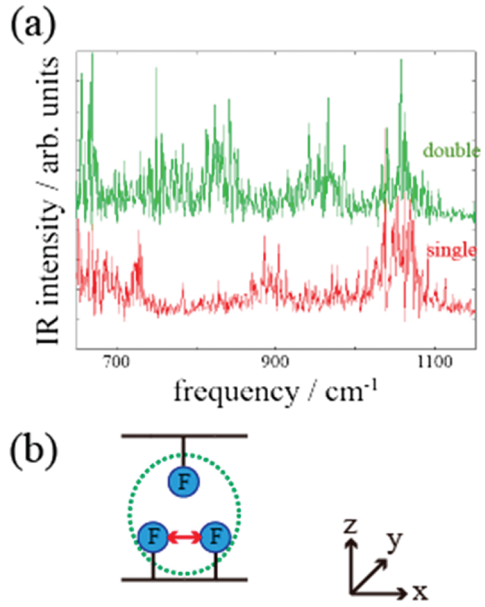

Figure 2. IR spectra computed in the 650−1150 cm^{-1} frequency range for the u fluorination pattern (Figure 1a). Light is polarized in the graphene plane and parallel to the fluorine chains (i.e., in the *x* direction; Figure 1d). The red and green lines describe the single- and double-layer structures. Part b schematically depicts the vibration along the *x* direction.

layer structure because the potential energy profile for the fluorine wagging motion becomes steeper as a result of interactions with the fluorines of the adjacent layer (Figure 2b).

The IR spectrum of triple-layer F−graphene is the sum of the spectra of the single- and double-layer cases, and the spectral profile for quadruple-layer F−graphene is very similar to that for the double-layer case (results not shown). These results indicate that fluorine atoms located on the opposite sides of adjacent graphene sheets, for example, layers 2 and 3 in Figure 1a, interact weakly. The 750 and 830 cm^{-1} peaks are seen in the triple- and quadruple-layer cases because both systems include at least one double-layer structure with the fluorine atoms facing each other. Thus, one can distinguish single- and multilayered u-fluorinated graphene structures by observing the peaks at 750 and 830 cm^{-1}.

The differences in the IR spectra between the single- and multilayer uudd-fluorinated graphene (Figure 1b) are illustrated in Figure 3. The light is polarized in the *y* direction perpendicular to the fluorine chains. Parts a and b of the figure focus on the low- and high-frequency parts, respectively, of the spectra. The multilayer structures can be most easily distinguished based on the IR peaks in the 650−950 cm^{-1} spectral region (Figure 3a). In particular, the 700 cm^{-1} peak disappears in the double-layer case, whereas it remains strong in the single- and triple-layer systems. The peak becomes optically inactive because the relevant vibrational motions in the adjacent layers are out-of-phase, as illustrated in Figure 3c. The peak also disappears in the quadruple-layer case (result not shown), indicating that one can distinguish odd-layered uudd F−graphene samples from even-layered samples by the existence of the 700 cm^{-1} peak. The same tendency is observed for the F−C(sp^3) wagging vibration at 880 cm^{-1} (Figure 3a).

The number of layers in odd-layer structures can be determined by the splitting of the 700 cm^{-1} peak due to interlayer interactions. The triple layer exhibits two additional

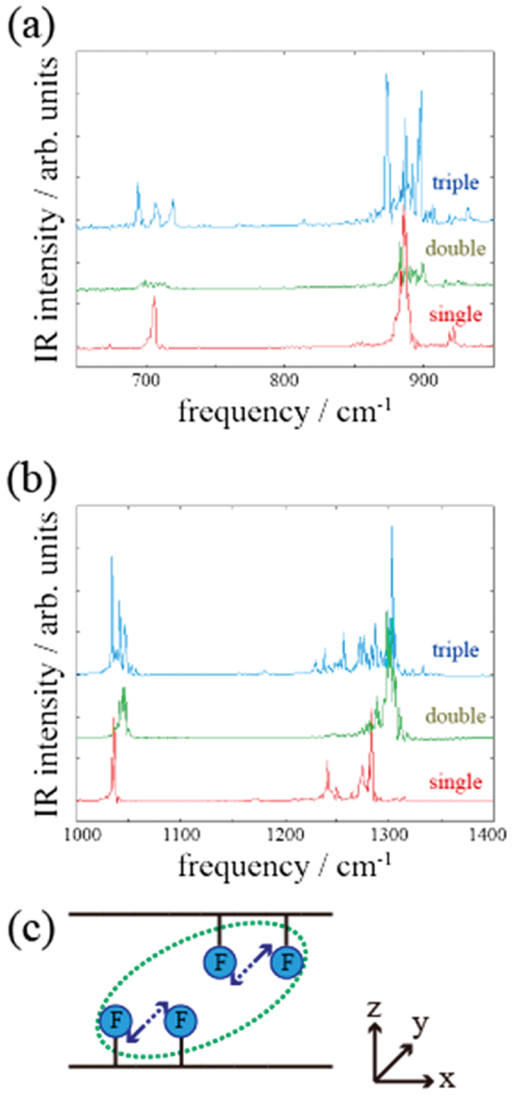

Figure 3. IR spectra for the uudd fluorination pattern (Figure 1b). Parts a and b focus on the 650−950 and 1000−1400 cm^{-1} frequency ranges, respectively. Light is polarized in the graphene plane and perpendicular to the fluorine chains (i.e., in the *y* direction; Figure 1d). The red, green, and blue lines describe the single-, double-, and triple-layer structures, respectively. Part c schematically depicts the IR-inactive vibrations along the *y* direction.

peaks at 690 and 720 cm^{-1}. It remains to be seen whether larger odd-layer stacks of graphene will exhibit distinct higher-order splitting of the 700 cm^{-1} peak. The intensities and frequencies of the additional peaks in the IR spectra of multilayer uudd-fluorinated graphene will depend on the details of the interlayer interaction. The peak splitting can serve as a measure the interaction strength. The stronger and longer-range the interaction is, the higher the peak splitting order will be. By comparing the theoretical and experimental results, one will be able to characterize the accuracy of the long-range nonbonding part of the graphene interaction potential.

Considering the 1000−1400 cm^{-1} frequency range of the *y*-polarized IR spectra for uudd-fluorinated graphene (Figure 3b), we found that the peaks appearing in the triple-layer case are combinations of the peaks for the single- and double-layer systems. This is in contrast to the lower-energy peaks (Figure 3a), which exhibit new features in the triple-layer case. At the same time, the additivity of the single- and double-layer spectra

dx.doi.org/10.1021/jp301856q | J. Phys. Chem. C 2012, 116, 8343−8347

of uudd-fluorinated graphene in the 1000−1400 cm^{-1} frequency range is analogous to that in the lower-energy spectra for the u-fluorinated graphene discussed above. Thus, the effect of the interlayer interaction on the IR spectrum depends on both the fluorination pattern and the type of vibrational modes under consideration. Depending on both factors, the IR spectra of multilayer structures can either be sums of the IR spectra of the single- and double-layer systems or exhibit changes that are more complex, stemming from triple-layer and higher-order interlayer interactions.

Figure 4 shows the IR spectra for the single- and multilayer structures with the ud fluorination pattern (Figure 1c)

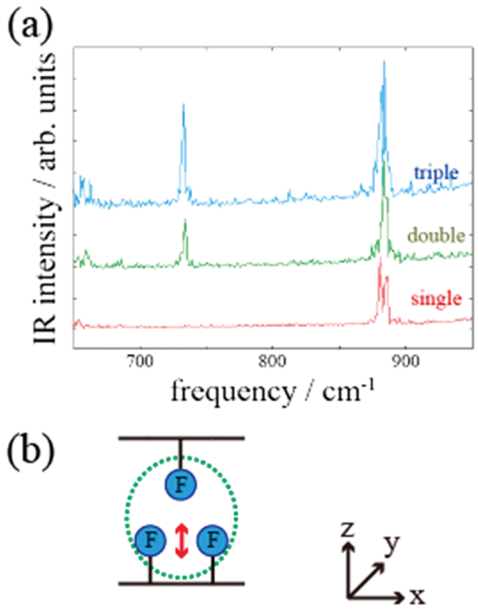

Figure 4. IR spectra computed in the 650−950 cm^{-1} frequency range for the ud fluorination pattern (Figure 1c). Light is polarized perpendicular to the graphene plane (i.e., in the z direction; Figure 1d). The red, green, and blue lines describe the single-, double-, and triple-layer structures, respectively. Part b schematically depicts the vibration along the z direction.

computed for light polarized in the z direction, perpendicular to the graphene plane. The spectra show that multilayered ud-fluorinated graphenes can be characterized using the 730 cm^{-1} peak. Absent in the monolayer, this peak arises from the interactions between adjacent layers (Figure 4b). The peak intensity grows with increasing number of layers, as illustrated in part a of Figure 4 for the single-, double-, and triple-layer systems. This trend continues for the quadruple-layer case (result not shown). Therefore, one can identify the number of layers in the multilayer ud F−graphene samples by analyzing the intensity of the 730 cm^{-1} peak in the IR spectrum. Further, by comparing the relative intensities of the 730 and 880 cm^{-1} peaks, one can characterize the strength of the interlayer interactions. The intensity of the latter peak is additive with respect to the number of layers, whereas the intensity of the former peak depends on the interlayer interaction strength. Such comparisons might prove valuable in designing and testing the long-range part of the graphene interaction potential for MD simulations.

Finally, we note that the three patterns, believed to be most important for fluorinated multilayered graphene,[1,6,20−22] were characterized above using different light polarizations, namely, x polarization for the u pattern, y polarization for the uudd pattern, and z polarization for the ud pattern (Figure 1). Therefore, the reported results will allow experimentalists to distinguish simultaneously both the pattern type and the number of graphene layers for each pattern.

4. CONCLUSIONS

In summary, by studying the IR spectra of multilayered fluorinated graphenes using molecular dynamics simulations, we have established specific signatures that identify the fluorination patterns and the number of layers in these systems. We have found that the peaks generated by the F−F vibrational modes that involve nearby fluorines in the same graphene layer are strongly influenced by interlayer interactions. Therefore, these peaks are most suitable for studying and describing the multilayer structures. The u fluorination patterns (Figure 1) are distinguished by appearance of 750 and 830 cm^{-1} bands in the x-polarized IR spectrum. The uudd fluorination is best described by the properties of the 700 cm^{-1} peak in the y-polarized spectrum. The ud pattern is sensitive to the 730 cm^{-1} F−F vibrational peak arising in the z-polarized spectrum.

The fluorinated graphene nanostructures considered in this study were simulated under ideal conditions. Experimental systems contain defects and isomers and are generally more complex. The rapid and exciting progress in the fluorination procedures[6,11,13,15,19] is leading to better-defined systems. The reported results indicate that IR spectroscopy is a valuable tool for structural and chemical characterization of halogenated multilayered graphene and related materials. The established IR spectral signatures of the commonly encountered fluorinated graphenes can guide experimentalists in their synthetic efforts to create useful and well-characterized graphene derivatives.

AUTHOR INFORMATION

Corresponding Author

*E-mail: prezhdo@chem.rochester.edu. Tel.: (+585)276-5664. Fax: (+585)276-0205.

Notes

The authors declare no competing financial interest.

ACKNOWLEDGMENTS

The authors thank Daniel Packwood for useful comments. A.U. is supported by the research fellowship of the Global COE Program, International Center for Integrated Research, and Advanced Education in Material Science, Kyoto University. Y.T. is grateful for the financial support in the form of a Grant-in-Aid for Scientific Research B19350011 from the Japan Society for the Promotion of Science. O.V.P. acknowledges the support of the United States as a Foreign Scholar of the Japan Society for the Promotion of Science and Grant CHE-1035196 from the National Science Foundation of the United States.

REFERENCES

(1) Dresselhaus, M. S.; Dresselhaus, G. *Adv. Phys.* **1981**, *30*, 139−326.

(2) Ang, P. K.; Wang, S.; Bao, Q.; Thong, J. T. L.; Loh, K. P. *ACS Nano* **2009**, *3*, 3587−3594.

(3) Robinson, J. T.; Burgess, J. S.; Junkermeier, C. E.; Badescu, S. C.; Reinecke, T. L.; Perkins, F. K.; Zalalutdniov, M. K.; Baldwin, J. W.; Culbertson, J. C.; Sheehan, P. E.; Snow, E. S. *Nano Lett.* **2010**, *10*, 3001−3005.

(4) Withers, F.; Bointon, T. H.; Dubois, M.; Russo, S.; Craciun, M. F. *Nano Lett.* **2011**, *11*, 3912−3916.

(5) Liang, Q.; Yao, X.; Wang, W.; Liu, Y.; Wong, C. P. *ACS Nano* **2011**, *5*, 2392−2401.
(6) Gupta, V.; Nakajima, T.; Ohzawa, Y.; Zemva, B. *J. Fluorine Chem.* **2003**, *120*, 143−150.
(7) Kazunari, Y.; Yumura, T.; Yamabe, T.; Bandow, S. *J. Am. Chem. Soc.* **2000**, *122*, 11871−11875.
(8) Tasis, D.; Tagmatarchis, N.; Bianco, A; Prato, M. *Chem. Rev.* **2006**, *106*, 1105−1136.
(9) Fan, X.; Liu, L.; Kuo, J. L.; Shen, Z. *J. Phys. Chem. C* **2010**, *114*, 14939−14945.
(10) Kalugin, O. N.; Chaban, V. V.; Loskutov, V. V.; Prezhdo, O. V. *Nano Lett.* **2008**, *8*, 2126−2130.
(11) Kita, Y.; Watanabe, N.; Fujii, Y. *J. Am. Chem. Soc.* **1979**, *101*, 3832−3841.
(12) Okotrub, A. V.; Yudanov, N. F.; Chuvilin, A. L.; Asanov, I. P.; Shubin, Y. V.; Bulusheva, L. G.; Gusel'nikov, A. V.; Fyodorov, I. S. *Chem. Phys. Lett.* **2000**, *322*, 231−236.
(13) Muramatsu, H.; Kim, Y. A.; Hayashi, T.; Endo, M.; Yonemoto, A.; Arikai, H.; Okino, F.; Touhara, H. *Chem. Commun.* **2005**, *15*, 2002−2004.
(14) Shulga, Y. M.; Tien, T. C.; Huang, C. C.; Lo, S. C.; Muradyan, V. E.; Polyakova, N. V.; Ling, Y. C.; Loutfy, R. O.; Moravsky, A. P. *J. Electron Spectrosc. Relat. Phenom.* **2007**, *160*, 22−28.
(15) Kalita, G.; Adhikari, S.; Aryal, H. R.; Ghimre, D. C.; Afre, R.; Soga, T.; Sharon, M.; Umeno, M. *Physica E* **2008**, *41*, 299−303.
(16) Brzhezinskaya, M. M.; Muradyan, V. E.; Vinogradov, N. A.; Preobrajenski, A. B.; Gudat, W.; Vinogradov, A. S. *Phys. Rev. B* **2009**, *79*, 155439.
(17) Touhara, H.; Okino, F. *Carbon* **2000**, *38*, 241−267.
(18) Lee, Y. S. *J. Fluorine Chem.* **2007**, *128*, 392−403.
(19) Bulusheva, L. G.; Fedoseeva, Y. V.; Okotrub, A. V.; Flahaut, E.; Asanov, I. P.; Koroteev, V. O.; Yaya, A.; Ewels, C. P.; Chuvilin, A. L.; Felten, A.; Van Lier, G.; Vyalikh, D. V. *Chem. Mater.* **2010**, *22*, 4197−4203.
(20) Kawasaki, S.; Komatsu, K.; Okino, F.; Touhara, H.; Kataura, H. *Phys. Chem. Chem. Phys.* **2004**, *6*, 1769−1772.
(21) Leenaerts, O.; Peelaers, H.; Hernandez-Nieves, A. D.; Partoens, B.; Peeters, F. M. *Phys. Rev. B* **2010**, *82*, 195436.
(22) Sahin, H.; Topsakal, M.; Ciraci, S. *Phys. Rev. B* **2011**, *83*, 115432.
(23) Kelly, K. F.; Chiang, I. W.; Mickelson, E. T.; Hauge, R. H.; Margrave, J. L.; Wang, X.; Scuseria, G. E.; Radloff, C.; Halas, N. J. *Chem. Phys. Lett.* **1999**, *313*, 445−450.
(24) Bettinger, H. F.; Kudin, K. N.; Scuseria, G. E. *J. Am. Chem. Soc.* **2001**, *123*, 12849−12856.
(25) Jaffe, R. L. *J. Phys. Chem. B* **2003**, *107*, 10378−10388.
(26) Lier, G. V.; Ewels., C. P.; Zuliani, F.; Vita, A. D.; Charlier, J. C. *J. Phys. Chem. B* **2005**, *109*, 6153−6158.
(27) Osuna, S.; Torrent-Sucarrat, M.; Sola, M.; Geerlings, P.; Ewels, C. P.; Lier, G. V. *J. Phys. Chem. C* **2010**, *114*, 3340−3345.
(28) Wu, M.; Tse, J. S.; Jiang, J. Z. *J. Phys. Chem. Lett.* **2010**, *1*, 1394−1397.
(29) Ueta, A.; Tanimura, Y.; Prezhdo, O. V. *J. Phys. Chem. Lett.* **2010**, *1*, 1307−1311.
(30) Ueta, A.; Tanimura, Y.; Prezhdo, O. V. *J. Phys. Chem. Lett.* **2012**, *3*, 246−250.
(31) Brenner, D. W. *Phys. Rev. B* **1990**, *42*, 9458−9471.
(32) Tanaka, J.; Abrams, C. F.; Graves, D. B. *J. Vac. Sci. Technol. A* **2000**, *18*, 938−945.
(33) Che, J.; Cagin, T.; Goddard 3, W. A. *Theor. Chem. Acc.* **1999**, *102*, 346−350.
(34) Parra, R. D.; Zeng, X. C. *J. Mol. Struct. (THEOCHEM)* **2000**, *503*, 213−220.
(35) Rohrer, J.; Hyldgaard, P. *Phys. Rev. B* **2011**, *83*, 165423.